Journal of the Meteorological Society of Japan

EARLY ONLINE RELEASE

The DOI for this manuscript is
DOI:10.2151/jmsj.2022-021
J-STAGE Advance published date: December 28th, 2021
The final manuscript after publication will replace the preliminary version at the above DOI once it is available.

Did Atmospheric CO_2 and CH_4 Observation at Yonagunijima Detect Fossil-Fuel CO_2 Reduction due to COVID-19 Lockdown?

Yasunori TOHJIMA[1], Yosuke NIWA

National Institute for Environmental Studies
Tsukuba, Japan

Kazuhiro TSUBOI

Meteorological Research Institute
Tsukuba, Japan

and

Kazuyuki SAITO

Japan Meteorological Agency
Tokyo, Japan

October 5, 2021

----

1) Corresponding author: Yasunori Tohjima, National Institute for Environmental Studies, Earth System Division, Environmental Chemodynamics Section, 16-2 Onogawa, Tsukuba 305-8506, Ibaraki, JAPAN
Email: tohjima@nies.go.jp
Tel: +81-29-850-2485
Fax: +81-3-6453-0612

Abstract

Synoptic-scale variabilities of atmospheric CO_2 and CH_4 observed at Yonagunijima (Yonaguni Island, YON, 24.47°N, 123.01°E) during winter (from January to March) in 1998-2020 were examined. The monthly mean variability ratios ($\Delta CO_2/\Delta CH_4$) based on correlation slopes within 24-hour time windows showed a clear increasing trend, which is mainly attributed to the unprecedented increase in the fossil fuel-derived CO_2 ($FFCO_2$) emissions from China. A similar increasing trend of the $\Delta CO_2/\Delta CH_4$ ratio had been reported for the observation at Hateruma Island (HAT, 24.06°N, 123.81°E), located at about 100 km east of YON. However, the absolute values for YON were 34% larger than those for HAT. In addition, the monthly average in February 2020 for YON showed no marked change, while that for HAT showed an abrupt considerable decrease associated with the $FFCO_2$ emission decrease in China presumably caused by the COVID-19 lockdown. Investigating the diurnal variations, we found that the local influences were larger at YON, especially during daytime, than at HAT. Using nighttime data (20-6 LST) and a longer time window (84-hour), we succeeded in reducing the local influences and the resulting monthly mean $\Delta CO_2/\Delta CH_4$ ratio showed considerable similarity to that observed at HAT including the abrupt decrease in February 2020. These results convinced us that the $\Delta CO_2/\Delta CH_4$ ratio could be successfully used to investigate the relative emission strength in the upwind region.

Keywords atmospheric CO_2; atmospheric CH_4; synoptic-scale variation; COVID-19

1. Introduction

In December 2019, the novel coronavirus disease (COVID-19) was first reported in Wuhan, China, and rapidly spread across the whole country. The government of China imposed lockdown measures first in Wuhan on 23 January 2020, then extended the area across the nation in February 2020. Since such lockdown measures strictly restricted socioeconomic activities, a considerable reduction in fossil fuel-derived CO_2 ($FFCO_2$) emissions was expected (Le Quéré et al., 2020). This situation raised the question of whether atmospheric observations could detect the COVID-19-induced $FFCO_2$ reductions.

Substantial reductions in air pollutants like nitrogen dioxide (NO_2) were observed during the lockdown period in China by using in-situ and satellite measurements (e.g., Bauwens et al., 2020; Le et al., 2020). However, the corresponding change in atmospheric CO_2 mole fraction was expected to be relatively small because of its rather long lifetime in comparison with the above air pollutants. Satellite retrievals of the CO_2 column average (XCO_2) over China were examined by several studies to detect the influence of the COVID-19 lockdown (Chevallier et al., 2020; Buchwitz et al., 2021), which concluded that the detection was challenging because the expected change of XCO_2 was less than the precision of the satellite observations.

Examining synoptic-scale variations in the atmospheric CO_2 and CH_4 observed at

Hateruma Island (HAT, 24.06°N, 123.81°E), Tohjima et al. (2020) found that the $\Delta CO_2/\Delta CH_4$ variability ratio showed a marked decrease in February 2020 compared with the former 9-year (2011-2019) average. Because HAT is in the downwind region of continental Asia during the late autumn - early spring season because of the East Asian monsoon, correlative elevations of the CO_2 and CH_4 mole fractions are often observed (Tohjima et al. 2010). A previous study revealed that the gradual increase of the $\Delta CO_2/\Delta CH_4$ ratio was attributed to the unprecedented increase in the $FFCO_2$ emissions from China (Tohjima et al., 2014). Consequently, Tohjima et al. (2020) concluded that the observed $\Delta CO_2/\Delta CH_4$ decrease in February 2020 was related to the COVID-19 lockdown in China. Moreover, they evaluated the decrease in the $FFCO_2$ emissions from China to be about 32 ± 12 % and 19 ± 15 % for February and March, respectively, from a comparison of the observed and simulated $\Delta CO_2/\Delta CH_4$ ratios. However, the change in the $\Delta CO_2/\Delta CH_4$ ratio associated with the COVID-19 was considerably faint and was detected only in single-site observations, limiting the certainty of the estimate of emission change. Therefore, to enhance the certainty, an independent observation is required.

Yonaguni Island (YON, 24.47°N, 123.01°E), where atmospheric CO_2 and CH_4 have also been observed by the Japan Meteorological Agency (JMA) since 1997 and 1998, respectively, is located at about 100 km west of HAT. The observed seasonal cycles and trends for HAT and YON were almost identical (Zhang, et al., 2007) because of the similarity of the geographical positions. Therefore, it is expected that the CO_2 and CH_4 observations at YON can be used to constrain the relative emission strengths from China. In this study, we examined whether the $\Delta CO_2/\Delta CH_4$ ratio observed at YON showed similar variations, especially an abrupt decrease in February 2020, as the observations at HAT did.

2. Data and Method

2.1 Yonagunijima (YON)

Yonagunijima (Yonaguni Island), located at the western end of the Ryukyu Archipelago, is the westernmost inhabited island of Japan. The island has a shape of an almond (longer in the east-west direction), an area of about 29 km^2 with the highest point being 231 m, and a population of about 1700. There are mountainous areas in the southern and western parts of the island, covered by subtropical forests. JMA built a local meteorological station to the east of the north settlement and about 800 m inland from the north coast in 1989. The station is surrounded by grassland and sugarcane fields. The observation at YON is generally influenced by the air masses from the Pacific region during summer and from the Asian continent during winter. Such seasonality in the air mass transport also influences the observation at HAT. Note that no clear diurnal patterns in wind direction and wind speed were observed at YON.

2.2 CO_2 and CH_4 measurement systems

The atmospheric CO_2 and CH_4 measurement systems used at YON are briefly described here; the details were presented elsewhere (e.g., Watanabe et al., 2000; Tsutsumi et al., 2006). The sample air was drawn by a pump from an air intake located at the top of a mast near the station building (20 m above ground level) and was delivered to the CO_2 and CH_4 measurement systems.

The CO_2 in the air sample was measured by using non-dispersive infrared analyzers (NDIRs). The analytical precisions of the NDIRs were better than ±0.02 μmol per mol (ppm). The CH_4 mole fractions were measured by a NDIR during January 1998 - December 2007 and by a gas chromatograph equipped with a flame ionization detector (GC/FID) after January 2008. The precisions of the atmospheric CH_4 measurement systems were better than ±10 nmol per mol (ppb) for the NDIR system and ±5 ppb for the GC/FID system.

The CO_2 and CH_4 measurement systems were calibrated by introducing working standard gases from high-pressure cylinders, which were prepared at the laboratory in JMA (Watanabe et al., 2000; Matsueda et al., 2018). The CO_2 and CH_4 mole fraction values at YON were reported on the WMO scale. Note that although the CO_2 and CH_4 mole fractions at HAT were reported on the NIES original scales, it was confirmed from the WMO/IAEA Round Robin comparison experiment (e.g., Zhou et al. 2009) that the differences between the WMO and NIES scales were kept within ±0.15 ppm.

2.3 Analytical methods of the variability ratio

The time series of CO_2 and CH_4 at YON often showed correlative synoptic-scale variations. To extract the variability ratios from such correlative variations, we used the same method as Tohjima et al., (2014; 2020) used to calculate the variability ratios for the observation at HAT. Since the details of the methods are given in the literature, here we give only a brief description of the methods.

First, using a set of the hourly CO_2 and CH_4 data within a certain time window, we computed a correlation coefficient (R), standard deviations for both CO_2 and CH_4 (σ_{CO2} and σ_{CH4}), and a correlation slope by using a reduced major axis (RMA) method (Hirsch and Gilroy, 1984). Shifting the time window by one hour, we repeated the above computations for the entire data set. Then, setting the criteria of the correlation coefficient (R) and the CO_2 standard deviation (σ_{CO2}), we discarded the correlation slopes with R and σ_{CO2} less than the criteria. Finally, using the selected correlation slopes, we calculated the monthly average and the moving averages of the variability ratio. Although the time window was set to 24 hours in Tohjima et al. (2020), we also tried a longer time period up to 120 hours in this study. Note that we used the same R=0.7 and σ_{CO2}=0.1 ppm for the criteria as were used in a previous study (Tohjima et al., 2020).

3. Results and Discussion

3.1 Synoptic-scale variations of the atmospheric CO_2 and CH_4

The time series of the hourly CO_2 and CH_4 mole fractions at YON from January to February 2020 and those observed at HAT are plotted in Fig. 1. Both CO_2 and CH_4 time series show similar synoptic-scale variations with periods of several hours to several days. The synoptic-scale variations observed at YON were almost the same as those observed at HAT except for phase differences; the temporal variations at YON generally proceed a few hours ahead of those at HAT. In addition, the CO_2 short-term variations observed at YON seem to be slightly larger than those at HAT.

We calculated the average diurnal cycles of CO_2 and CH_4 at YON and HAT for three months (Jan.-Mar.) to clarify the differences (Fig. 2). The average diurnal cycle is calculated as the average deviation from the corresponding daily means for the individual hours. Although CO_2 diurnal cycles showed a decline during daytime at both sites, the amplitudes of the decline for YON are more than twice as large as those for HAT. The declines during daytime are probably attributed to the photosynthetic CO_2 sequestrations of the biosphere on the islands. These results suggest that the local CO_2 fluxes more strongly influence the atmospheric observation at YON than at HAT. The larger local influence at YON may be attributed to the fact that the station at YON is located in a more inland area of the larger island and partially that the sampling inlet is placed at a lower position.

Meanwhile, compared with the analytical precision of the CH_4 measurements (±2 ppb for HAT (Tohjima et al., 2002)), the ranges of the average CH_4 diurnal cycles of ±1.5 ppb and ±1 ppb for YON and HAT, respectively, are relatively small. These results suggest that the influence of the local sources on the observed atmospheric CH_4 variations is negligible for both sites.

3.2 **Temporal change in the monthly mean $\Delta CO_2/\Delta CH_4$ ratio**

Monthly mean $\Delta CO_2/\Delta CH_4$ ratios based on the observation at YON in January, February, and March from 1998 to 2020 are plotted in Fig. 3a together with the $\Delta CO_2/\Delta CH_4$ ratios for HAT, reported in a previous study (Tohjima et al., 2020). As the figure shows, the $\Delta CO_2/\Delta CH_4$

ratios for YON are 39 mol mol^{-1} on average larger than those for HAT (averages of 156 mol mol^{-1} for YON and 117 mol mol^{-1} for HAT). In addition, the increasing ratios determined by linear regression for the entire period (1998-2020) are larger for YON (3.2 ± 0.3 mol mol^{-1} yr^{-1}) than for HAT (1.9 ± 0.2 mol mol^{-1} yr^{-1}). The smaller increasing trend at HAT may be related to the fact that the $\Delta CO_2/\Delta CH_4$ ratio for HAT reached a plateau after 2011 in association with the stagnant $FFCO_2$ emission increase from China (see Fig.2 of Tohjima et al., 2020). The increasing rate for HAT decreased from 2.7 ± 0.4 mol mol^{-1} yr^{-1} in 1998-2010 to −0.6 ± 0.7 mol mol^{-1} yr^{-1} after 2010, while that for YON for the later period was 3.7 ± 0.7 mol mol^{-1} yr^{-1}.

Considering the relatively close geographical locations of YON and HAT, it is quite difficult to imagine that the air masses transported from continental Asia induce such considerably large differences between YON and HAT. Therefore, the larger short-term variability probably caused by the local CO_2 fluxes would explain the larger $\Delta CO_2/\Delta CH_4$ ratios for YON. The average diurnal cycles of CO_2 at YON (Fig. 2) show rather stable values during nighttime but rapid decreases and increases during daytime, which might indicate an enhancement of the short-term variability during daytime. To investigate the difference in the short-term variability of CO_2 for YON between daytime and nighttime, we computed the frequency distributions of the standard deviations of the CO_2 data within the 24-hour time windows for the daytime (7-19LST) and nighttime (20-6LST). The result showed that the peak of the frequency distribution was located at a larger standard deviation for the daytime data than for the nighttime data (supplementary Fig. S1). Accordingly, there is a possibility that the daytime data might enlarge the $\Delta CO_2/\Delta CH_4$ ratios for YON.

3.3 Reduction of local influences

To reduce the local influences on the observations at YON, we calculated the monthly $\Delta CO_2/\Delta CH_4$ ratio by only using nighttime data (supplementary Fig. S2). Although the resulted monthly means decreased by about 20 mol mol^{-1} on average, those values were still about 19 mol/mol larger than the values for HAT, suggesting the local influence was still not sufficiently reduced. To further reduce the local influences, we used a rather long time window for the correlation analysis. As was discussed in the previous sections, the local influences appeared in the diurnal cycles, while the synoptic-scale variations usually had a longer timescale of several days. Therefore, the longer time window could reduce the influence of the local CO_2 fluxes on the total CO_2 variations. Thus, we calculated the monthly $\Delta CO_2/\Delta CH_4$ ratios for YON for different time windows up to 120 hours and examined the root mean square (RMS) of the differences of the monthly $\Delta CO_2/\Delta CH_4$ ratios between YON and HAT (supplementary Fig. S3). The RMS showed a minimum value when an 84-hour time window was used. The result using the 84-hour time window is plotted in Fig. 3b. The modified $\Delta CO_2/\Delta CH_4$ ratios are similar to the $\Delta CO_2/\Delta CH_4$ ratios for HAT; the average difference (YON−HAT) is −2 mol mol^{-1}. The increasing rates determined by the linear regression were 3.7 ± 0.7 mol mol^{-1} yr^{-1} during 1998-2010 and 0.1 ± 0.8 mol mol^{-1} yr^{-1} during 2011-2020, which are also consistent with those for HAT.

Moreover, the modified $\Delta CO_2/\Delta CH_4$ ratio for YON showed a substantial decrease in February 2020. As is described in the Introduction, Tohjima et al. (2020) attributed the decrease in the monthly $\Delta CO_2/\Delta CH_4$ ratio in February and March 2020 from the preceding 9-year averages to the decrease in the $FFCO_2$ emissions from China associated with the COVID-19-induced lockdown. The monthly averages of the modified $\Delta CO_2/\Delta CH_4$ ratio for YON and the previously reported corresponding values for HAT are listed in Table 1 for comparison. Note that the duration of the time window also influenced the $\Delta CO_2/\Delta CH_4$ ratios for HAT as suggested by Tohjima et al. (2020) and the February $\Delta CO_2/\Delta CH_4$ ratios for HAT decreased to 22 mol mol^{-1} when the 84-hour time window and the nighttime data were used. Even if the influence of the duration of the time window is considered, the decreases in the $\Delta CO_2/\Delta CH_4$ ratio for YON agree well with those for HAT within the uncertainties both for February and March. Although the decrease in March for YON is unclear in comparison with that for HAT, using a 120-hour time window enlarges the decrease to 10 mol mol^{-1}, which suggests that it is difficult to completely reduce local influences.

Figure 4 shows the temporal variation in the 30-day moving average of the modified $\Delta CO_2/\Delta CH_4$ ratio for YON from January to March 2020. In the figure, the preceding 9-year (2011-2019) average of the 30-day moving average for YON with the range of the uncertainties (1σ) and the 30-day moving average of the $\Delta CO_2/\Delta CH_4$ ratio for HAT from January to March 2020, which were shown in Fig. 3 of Tohjima et al. (2020), are also depicted. Compared with the preceding 9-year average, the moving-averaged $\Delta CO_2/\Delta CH_4$

ratio for YON shows a rapid decrease between January and February, a bottom in the middle of February, and an asymptotic increase toward the 9-year average. Such variations are generally consistent with those for HAT. Additionally, the pattern of variations in the moving-averaged $\Delta CO_2/\Delta CH_4$ ratio is similar to the estimated change in the $FFCO_2$ emissions from China based on Le Quéré et al., (2020) which is also depicted in Fig. 4.

From the above results, we concluded that the atmospheric CO_2 and CH_4 observations at YON could detect the signals related to the COVID-19 lockdown in China as the change in the $\Delta CO_2/\Delta CH_4$ ratio. This conclusion supports the idea that the atmospheric $\Delta CO_2/\Delta CH_4$ ratio is effective in evaluating temporal changes in the relative emission strengths in the up-wind source regions.

4. Summary and Conclusion

To detect the signal associated with the COVID-19 lockdown, we examined the synoptic-scale variability ratio of the atmospheric CO_2 and CH_4 ($\Delta CO_2/\Delta CH_4$) observed at YON during the period from 1998 to 2020 by applying the analytical approach of Tohjima et al. (2020). Being different from the results observed at HAT (Tohjima et al., 2020), the $\Delta CO_2/\Delta CH_4$ ratio was about 34% larger than that for HAT, and the $\Delta CO_2/\Delta CH_4$ ratio for February 2020 did not show a marked decrease. Examining the diurnal variations of CO_2 and CH_4 at YON, we found that the local fluxes, probably air-to-land biosphere exchange, enhanced the CO_2 variability especially during daytime (7-19 LST).

Using the nighttime (20-6 LST) data and a longer time window of 84 hours, we were able to effectively reduce the local influences on the $\Delta CO_2/\Delta CH_4$ ratios; the resulting monthly $\Delta CO_2/\Delta CH_4$ ratios showed considerable agreement with those for HAT, including a marked decrease in February 2020 in comparison with the preceding 9-year (2011-2019) averages. Additionally, the 30-day moving average of the $\Delta CO_2/\Delta CH_4$ ratio abruptly decreased between January and February 2020, reached the bottom in the middle of February, and gradually returned to the level of the former 9-year average in March. Such a decline pattern is similar to the change in the $FFCO_2$ emissions from China estimated based on the study of Le Quéré et al. (2020).

As is described in the Introduction, detecting the decrease in the atmospheric CO_2 related to the COVID-19 outbreak is still challenging (Chevallier et al., 2020; Buchwitz et al., 2021). The change in the $\Delta CO_2/\Delta CH_4$ ratio at HAT associated with the COVID-19 outbreak is also very faint. Therefore, the fact that a decrease in the $\Delta CO_2/\Delta CH_4$ ratio in February 2020 was observed at YON convinced us of the correctness of the previous result reported by Tohjima et al. (2020). This result also demonstrates the usefulness of utilizing adjacent monitoring sites like YON and HAT to confirm the detection of such faint signals as shown in this study. Both sites are located at the downwind side of the Asian continent that is the biggest CO_2 emitter in the world and hence the most important area to be monitored. Monitoring with observations at YON and HAT would continue to provide valid information on emission changes over the continent.

Data Availability Statement

The time series of the atmospheric CO_2 and CH_4 mole fractions at YON are available via the website of WDCGG (World Data Centre for Greenhouse Gases). WDCGG (World Data Centre for Greenhouse Gases) (kishou.go.jp)

Supplement

Supplement 1 shows the frequency distributions of the standard deviations for the daytime and nighttime CO2 data for YON. Supplement 2 shows the same figure as Fig. 3, but only nighttime data are used to calculate the monthly average of the $\Delta CO_2/\Delta CH_4$ ratios for YON. Supplement 3 shows the root mean square (RMS) of the differences of the monthly $\Delta CO_2/\Delta CH_4$ ratios between YON and HAT against the duration of the time window used for the calculation for YON.

Acknowledgments

We are grateful to many staff members of the Japan Meteorological Agency for their work in the long-term observations of atmospheric CO_2 and CH_4 at YON. This study was financially supported by funds provided by the Environment Research and Technology Development Fund (JPMEERF21S20802).

References

Bauwens, M., S. Compernolle, T. Stavrakou, J.-F. Muller, J. van Gent, H. Eskes, P. F. Levelt, R. van der A, J. P. Veefkind, J. Vlietinck, H. Yu, and C. Zehner, 2020: Impact of coronavirus outbreak on NO_2 pollution assessed using TROPOMI and OMI observations. *Geophys. Res. Lett.*, **47**, e2020GL087978, https://doi.org/10.1029/2020GL087978.

Buchwitz, M., M. Reuter, S. Noël, K. Bramstedt, O. Schneising, M. Hilker, B. F. Andrade, H. Bovensmann, J. P. Burrows, A. Di Noia, H. Boesch, L. Wu, J. Landgraf, I. Aben, C. Retscher, C. W. O'Dell, and D. Crisp, 2021: Can a regional-scale reduction of atmospheirc CO_2 during the COVID-19 pandemic be detected from space? A case study for East China using satellite XCO_2 retrievals. *Atmos. Meas. Tech.*, **14**, 2141-2166, https://doi.org/10.5194/amt-14-2141-2021.

Chevallier, F., B. Zheng, G. Broquet, P. Ciais, Z. Liu, S. J. Davis, Z. Deng, Y. Wang, F.-M. Bréon, and C. W. O'Dell, 2020: Local anomalies in the column-averaged dry air mole fractions of carbon dioxide across the globe during the first months of the coronavirus recession. *Geophys. Res. Lett.*, **47**, e2020GL090244, https://doi.org/10.1029/2020GL090244.

Hirsch, R. M., and E. J. Gilroy, 1984: METHODS OF FITTING A STRAIGHT LINE TO DATA: EXAMPLES IN WATER RESOURCES. *J. Am. Water Resour. Assoc.* **20**, 705–711 (1984).

Le, T., Y. Wang, L. Liu, J. Yang, Y. L. Yung, G. Li, and J. H. Seinfeld, 2020: Unexpected air pollution with marked emission reductions during the COVID-19 outbreak in China. *Science,* **369** (6504), 702-706, doi:10.1126/science.abb7431.

Le Quéré, C., R. B. Jackson, M. W. Jones, A. J. P. Smith, S. Abernethy, R. M. Andrew, A. J. De-Gol, D. R. Willis, Y. Shan, J. G. Canadell, P. Friedlingstein, F. Creutzig, and G. P. Peters, 2020: Temporary reduction in daily global CO_2 emissions during the COVID-19 forced confinement. *Nat. Clim. Chang*. doi:10.1038/s41558-020-0797-x.

Matsueda, H., K. Tsuboi, S. Takatsuji, T. Kawasaki, M. Nakamura, K. Saito, A. Takizawa, K .Dehara, and S. Hosokawa, 2018: Evaluation of a new methane calibration system at JMA for WCC Round Robin experiments. *Papers in Meteorology and Geophysics*, **67**, 57–67, doi:10.2467/mripapers.67.57.

Tohjima, Y., T. Machida, M. Utiyama, M. Katsumoto, Y. Fujinuma, and S. Maksyutov, 2002: Analysis and presentation of in situ atmospheric methane measurements from Cape Ochi-ishi and Hateruma Island. *J. Geophys. Res.*, **107**, D12, doi:10.1029/2001JD001003.

Tohjima, Y., P. K. Patra, Y. Niwa, H. Mukai, M. Sasakawa, and T. Machida, 2020: Detection of fossil-fuel CO_2 plummet in China due to COVID-19 by observation at Hateruma. *Sci. Rep.*, **10,** 18688, https://doi.org/10.1038/s41598-020-75763-6.

Tohjima, Y., H. Mukai, S. Hashimoto, and P. K. Patra, 2010: Increasing synoptic scale variability in atmospheric CO_2 at Hateruma Island associated with increasing East-Asian emissions. *Atmos. Chem. Phys.*, **10**, 453–462, doi:10.5194/acp-10-453-2010.

Tohjima, Y., M. Kubo, C. Minejima, H. Mukai, H. Tanimoto, A. Ganshin, S. Maksyutov, K. Katsumata, T. Machida, and K. Kita, 2014: Temporal changes in the emissions of CH_4 and CO from China estimated from CH_4 / CO_2 and CO / CO_2 correlations observed at Hateruma Island. *Atmos. Chem. Phys.*, **14**, 1663–1677, doi:10.5194/acp-14-1663-2014.

Tsutsumi, Y., K. Mori, M. Ikegami, T. Tashiro, and K. Tsuboi, 2006: Long-term trends of greenhouse gases in regional and background events observed during 1998-2004 at Yonagunijima located to the east of the Asian continent. *Atmos. Env.*, **40**, 5868-5879.

Watanabe, F., O. Uchino, Y. Joo, M. Aono, K. Higashijima, Y. Hirano, K. Tsuboi, and K. Suda, 2000: Interannual variation of growth rate of atmospheric carbon dioxide concentration observed at the JMA's three monitoring stations: large increase in concentration of atmospheric carbon dioxide in 1998. *J. Meteorol. Soc. Jpn.*, **78**, 673-682.

Zhang, X., T. Nakazawa, M. Ishizawa, S. Aoki, S. Nakaoka, S. Sugawara, S. Maksyutov, T. Saeki, and T. Hayasaka, 2007: Temporal variations of atmospheric carbon dioxide in the southernmost part of Japan. *Tellus B*, **59**, 654-663, https://doi.org/10.1111/j.1600-0889.2007.00288.x.

Zhou, L., D. Kitzis, and P. P. Tans, 2009: Report of the fourth WMO Round-Robin reference gas intercomparison, 2002-2007, in Report of the 14th WMO Meeting of Experts on Carbon Dioxide Concentration and Related Tracer Measurement Techniques, Helsinki, Finland, 10-13 September 2007, WMO/GAW Rep. 186, edited by: Laurila, T., 40-43, WMO, Genova, Switzerland.

List of Figures

Fig. 1 Time series of the hourly CO_2 (red line, left Y-axis) and CH_4 (blue line, right inverse Y-axis) mole fractions observed at YON from February to March 2020. The gray lines represent corresponding hourly mole fractions observed at HAT.

Fig. 2 Average diurnal cycles of (a) CO_2 and (b) CH_4 at YON (red lines) and HAT (black lines) for three months (January: triangles; February: circles; March: squares). The average diurnal cycle is calculated as the average deviation from the daily means for the individual hours.

Fig. 3 (a) Monthly mean $\Delta CO_2/\Delta CH_4$ ratios based on the observation at YON (red closed symbols) and HAT (black open symbols) for January (triangles), February (circles), and March (squares) from 1998 to 2020. The $\Delta CO_2/\Delta CH_4$ ratios for HAT are taken from Tohjima et al., (2020). A 24-hour time window was used to calculate the $\Delta CO_2/\Delta CH_4$ ratios both for YON and HAT. (b) Same as (a) but only nighttime data (20-6 LST) and an 84-hour time window were used to calculate the $\Delta CO_2/\Delta CH_4$ ratios for YON.

Fig. 4 (Top, left Y-axis) Temporal variations in the 30-day moving average of the modified $\Delta CO_2/\Delta CH_4$ ratio for YON (red) and HAT (blue) from January to March 2020. The $\Delta CO_2/\Delta CH_4$ ratios for YON are based on the nighttime data and an 84-hour time window to reduce the local influences (see text). The $\Delta CO_2/\Delta CH_4$ ratios for HAT were taken from a previous study (Fig. 3 of Tohjima et al., 2020). The grey line with vertical bars represents the preceding 9-year (2011-2019) average of the 30-day moving average for YON with the range of the uncertainties (1σ). (Bottom, right Y-axis): the estimated temporal change in the $FFCO_2$ emissions from China based on Le Quéré et al., (2020).

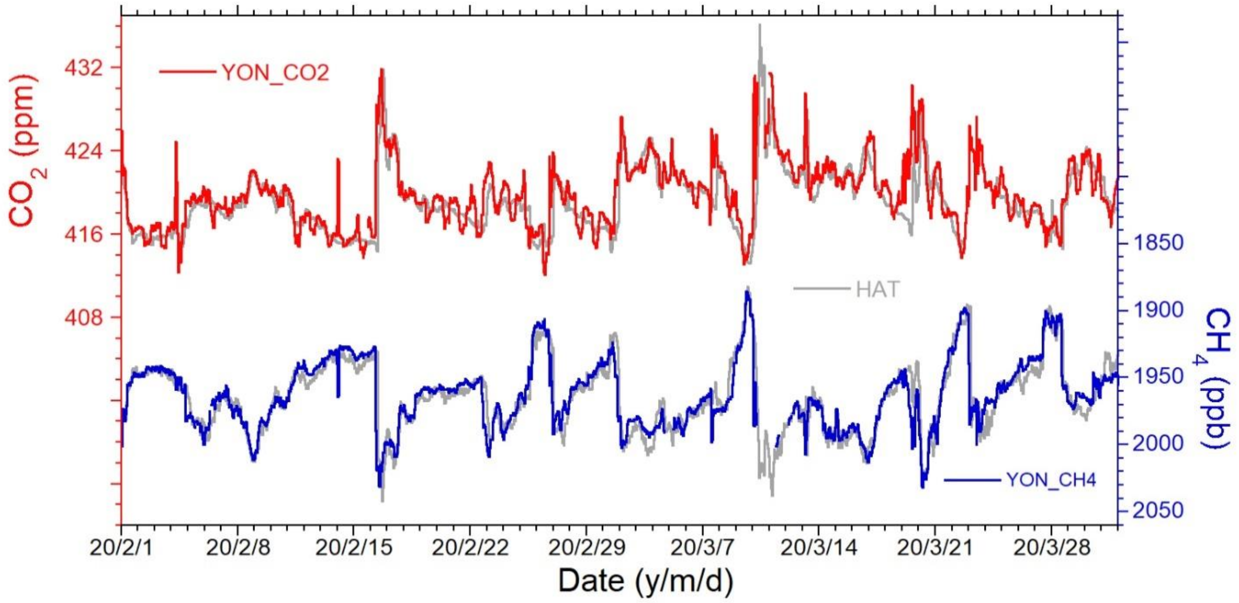

Fig. 1 Time series of the hourly CO_2 (red line, left Y-axis) and CH_4 (blue line, right inverse Y-axis) mole fractions observed at YON from February to March 2020. The gray lines represent corresponding hourly mole fractions observed at HAT.

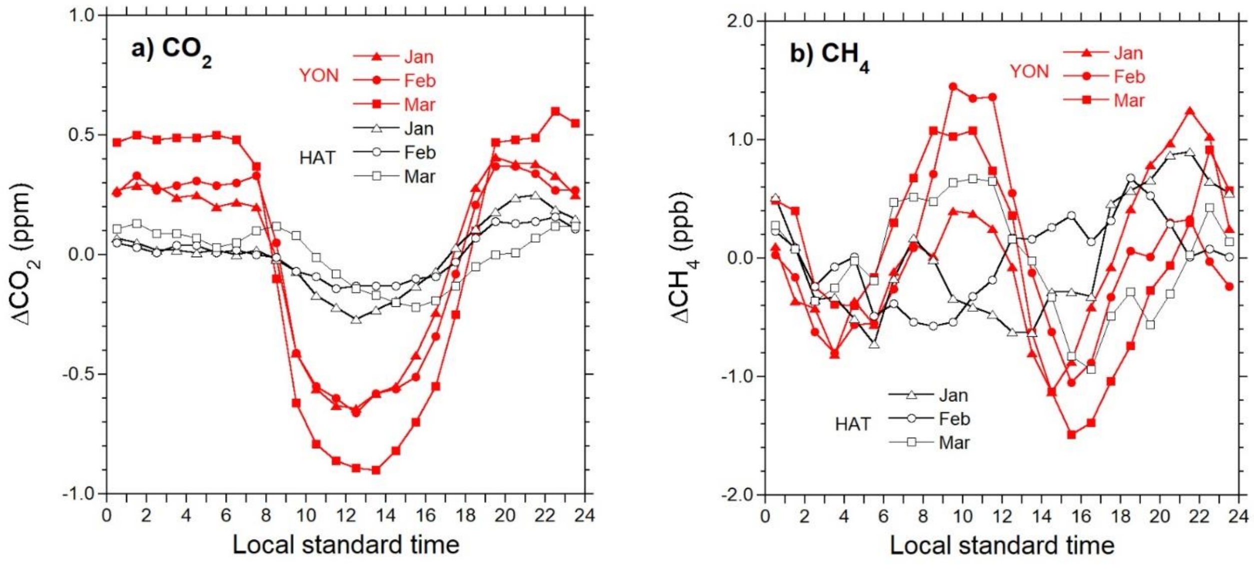

Fig. 2 Average diurnal cycles of (a) CO_2 and (b) CH_4 at YON (red lines) and HAT (black lines) for three months (January: triangles; February: circles; March: squares). The average diurnal cycle is calculated as the average deviation from the daily means for the

individual hours.

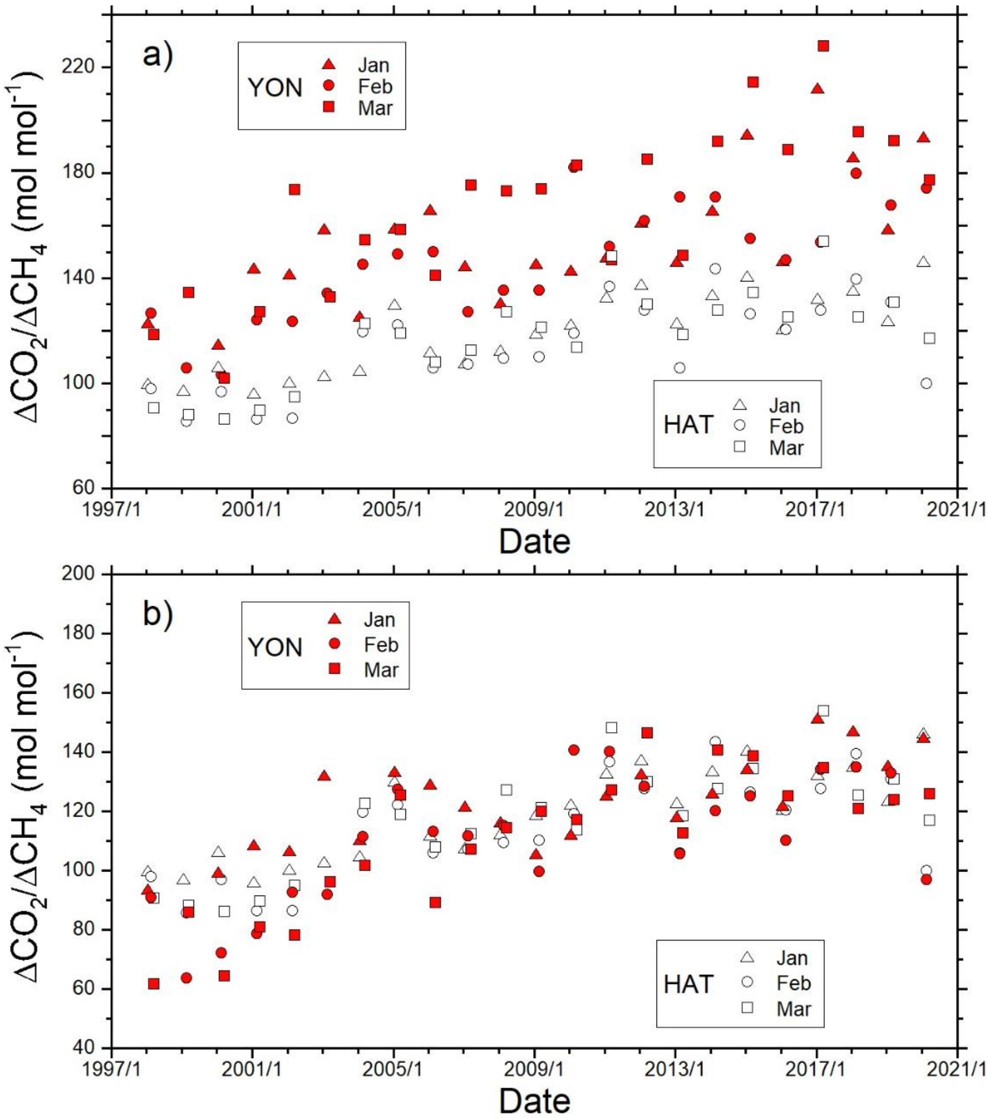

Fig. 3 (a) Monthly mean $\Delta CO_2/\Delta CH_4$ ratios based on the observation at YON (red close symbols) and HAT (black open symbols) for January (triangles), February (circles) and March (squares) from 1998 to 2020. The $\Delta CO_2/\Delta CH_4$ ratios for HAT are taken from Tohjima et al., (2020). A 24-hour time window was used to calculate the $\Delta CO_2/\Delta CH_4$ ratios both for YON and HAT. (b) Same as (a) but only nighttime data (20-6 LST) and an

84-hour time window were used to calculate the $\Delta CO_2/\Delta CH_4$ ratios for YON.

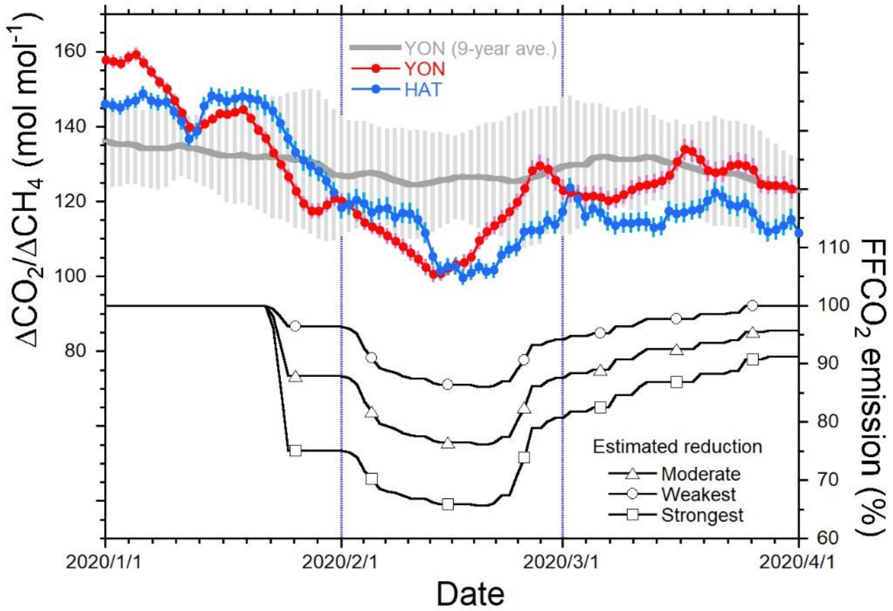

Fig. 4 (Top, left Y-axis) Temporal variations in the 30-day moving average of the modified $\Delta CO_2/\Delta CH_4$ ratio for YON (red) and HAT (blue) from January to March 2020. The $\Delta CO_2/\Delta CH_4$ ratios for YON are based on the nighttime data and an 84-hour time window to reduce the local influences (see text). The $\Delta CO_2/\Delta CH_4$ ratios for HAT were taken from a previous study (Fig. 3 of Tohjima et al., 2020). The grey line with vertical bars represents the preceding 9-year (2011-2019) average of the 30-day moving average for YON with the range of the uncertainties (1σ). (Bottom, right Y-axis): the estimated temporal change in the $FFCO_2$ emissions from China based on Le Quéré et al., (2020).

List of Tables

Table 1 Estimated changes in the monthly $\Delta CO_2/\Delta CH_4$ ratios in February and March 2020 from the preceding 9-year averages for YON and HAT[a] .

Site	Date	Monthly mean $\Delta CO_2/\Delta CH_4$[b]	Preceding 9-year average[c]	Decrease from the 9-year average
YON	February 2020	97 ± 2	126 ± 12	28 ± 12
YON	March 2020	126 ± 2	130 ± 11	4 ± 11
HAT	February 2020	100 ± 2[d]	129 ± 11[d]	29 ± 11
HAT	March 2020	117 ± 2[d]	133 ± 11[d]	16 ± 11

[a]Values are given in mol mol^{-1}.
[b]Uncertainties are standard errors of the corresponding monthly averages.
[c]Uncertainties are standard deviations of the corresponding 9-year averages.
[d]Values are taken from a previous study (see Table 1 of Tohjima et al., 2020).